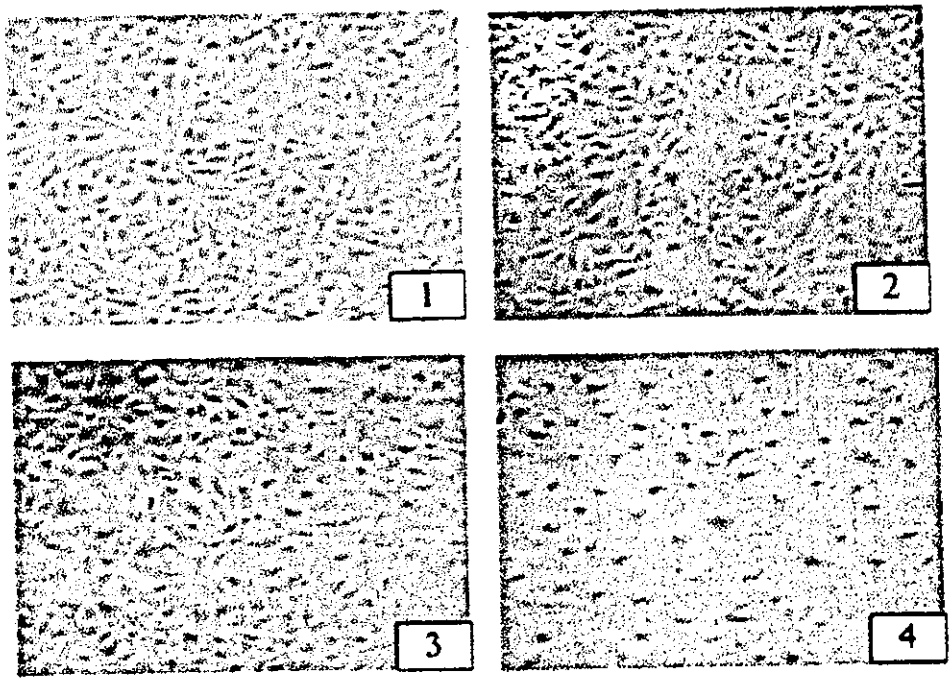

Figure 1. Morphologic change of HLE cells treated with natural IFN-α and sodium butyrate. As the result of treatment with natural IFN-α and sodium butyrate, the shape and size of HLE cells were changed. With the treatment of 1000 IU/ml of IFN-α for 7 days, the size of HLE cell became slightly larger and the morphology was round-shaped, although it hardly changed with 100 IU/ml of IFN-α. The treatment of HLE cells with 2 mM sodium butyrate changed the shape of cells more than that stimulated by IFN-α. Nucleic size of HLE cells became larger. 1, Control; 2, Cells treated with 100 IU/ml of IFN-α for 7 days; 3, Cells treated with 1000 IU/ml of IFN-α for 7 days; 4, Cells treated with 2 mM of sodium butyrate for 7 days. Original magnification x100.

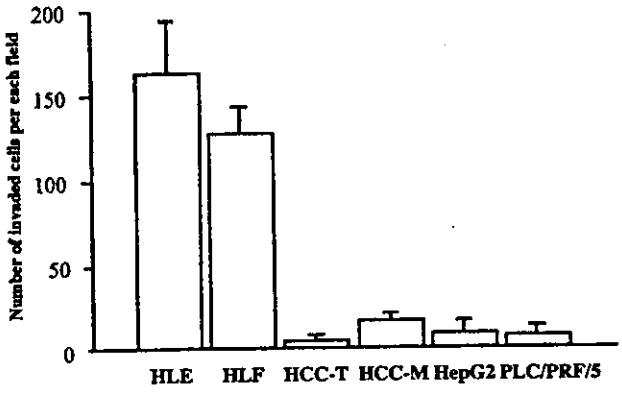

Figure 2. The morphometric analysis of the number of cells invaded from the upper-side chamber to the lower-side chamber in six human HCC cell lines. Invasion through Matrigel of HLE, HLF, HCC-T, HCC-M, HepG2 and PLC/PRF/5 was assayed using the Biocoat Matrigel Invasion Chamber. The cancer cells invade into the Matrigel, and appear on the lower surface of the Matrigel membrane. The number of invaded cells was counted in randomly selected 5 fields in every experiment (n=5).

showed that pro-MMP-2 and 9, and active MMP-2 and -9 were detected in the culture supernatants of both HLE and HLF. In HLE cells, production of MMP-2 was higher than that of MMP-9, and HLF produced much more MMP-9 than MMP-2. The culture supernatants of HLE and HLF treated with IFN-α (1000 IU/ml) and sodium butyrate (2 mM) for 7 days showed significant reduction of pro- and active-MMPs production in both cell lines. Especially MMP-2 activity almost disappeared by gelatin zymography in both cell lines (Fig. 4).

Effect of natural IFN-α and sodium butyrate on MMP-2 and -9 activities. Effect of agents on MMP activity was further examined using the MMP activity assay, which can detect active-form of MMP-2 and MMP-9. Active MMP-2 levels in HLE and HLF were 1.3±0.2 ng/ml and 0.5±0.2 ng/ml, respectively, in their control culture conditions. Active MMP-9 levels in HLE and HLF were 0.7±0.3 ng/ml and 1.2±0.3 ng/ml, respectively, in their control culture conditions. These levels almost disappeared by treatment with both IFN-α and sodium butyrate (Fig. 5).

Real-time quantitative RT-PCR assay. Effect of IFN-α and sodium butyrate on transcription of the MMP family and its counterpart, TIMP-1 and -2 was examined by real-time RT-PCR. The production of MMP-1 that dissolves type I collagen and promotes cancer cell invasion into its surrounding tissue was more or less inhibited by both agents. The mRNA levels of MMP-1 were slightly decreased by stimulation with 1000 IU/ml of IFN-α, and were significantly reduced by treatment with 2 mM of sodium butyrate. On the other hand, the agents variously changed the production of TIMP that inhibits MMP activity. The mRNA levels of TIMP-1 and TIMP-2, which are counterpart enzymes of MMP, were significantly increased by IFN-α ($p<0.01$, Mann-Whitney's U test) and slightly decreased by sodium butyrate (Fig. 6).

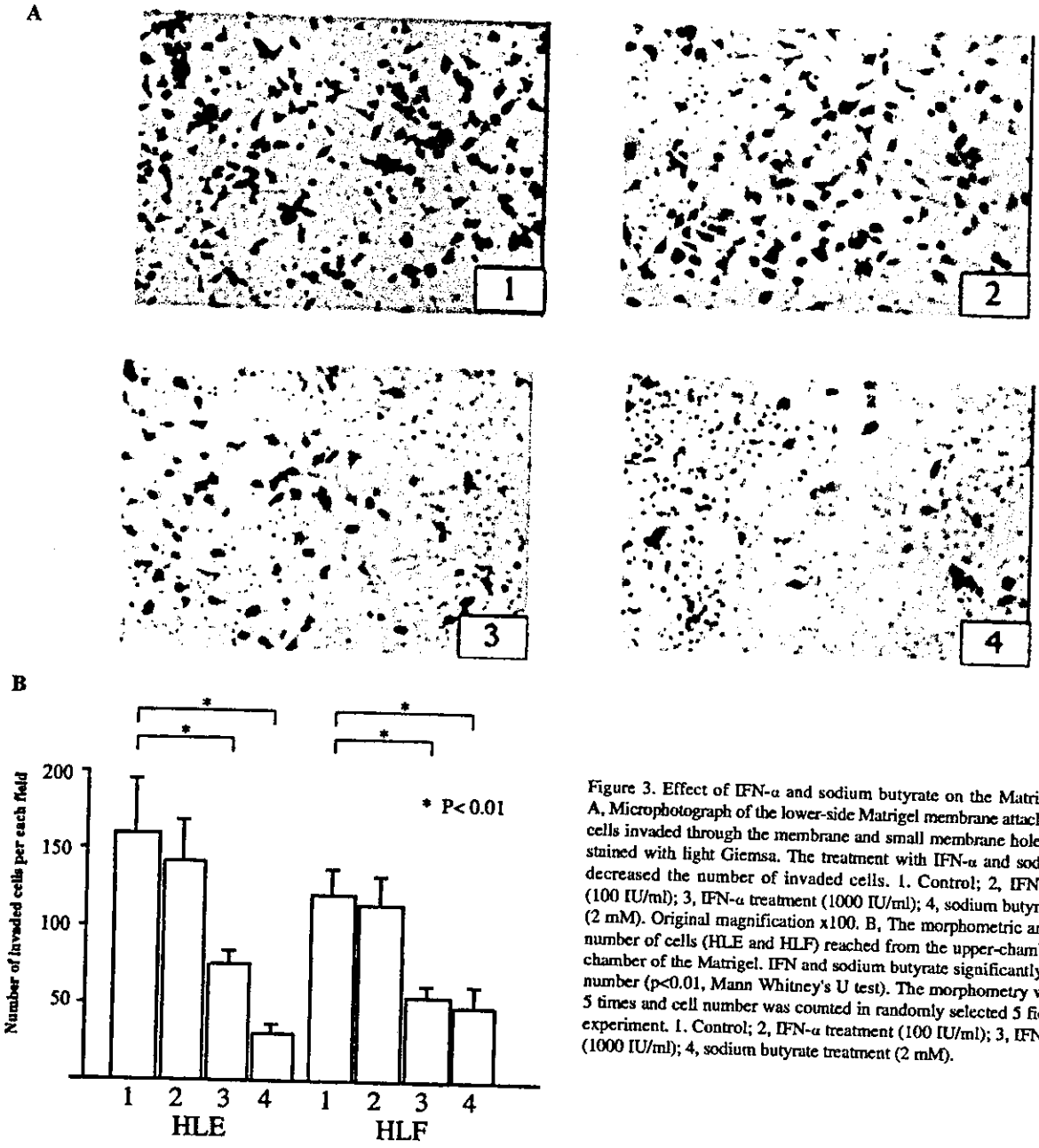

Figure 3. Effect of IFN-α and sodium butyrate on the Matrigel invasion. A, Microphotograph of the lower-side Matrigel membrane attached with HLE cells invaded through the membrane and small membrane holes. Cells were stained with light Giemsa. The treatment with IFN-α and sodium butyrate decreased the number of invaded cells. 1. Control; 2, IFN-α treatment (100 IU/ml); 3, IFN-α treatment (1000 IU/ml); 4, sodium butyrate treatment (2 mM). Original magnification x100. B, The morphometric analysis of the number of cells (HLE and HLF) reached from the upper-chamber to lower-chamber of the Matrigel. IFN and sodium butyrate significantly reduced the number ($p<0.01$, Mann Whitney's U test). The morphometry was achieved 5 times and cell number was counted in randomly selected 5 fields in every experiment. 1. Control; 2, IFN-α treatment (100 IU/ml); 3, IFN-α treatment (1000 IU/ml); 4, sodium butyrate treatment (2 mM).

Discussion

This study demonstrated that both IFN-α and sodium butyrate are potent inhibitors of malignancy of human HCC, especially of cellular invasive activity. Type I IFN has various anti-cancer activities, such as anti-proliferative activity, immuno-modulatory activity, and anti-angiogenic activity (37), in addition to anti-viral activity, and it has been clinically used in patients with renal cell carcinoma, multiple myeloma, chronic myelocytic leukemia, and hairy cell leukemia. Anti-malignant effect of IFN has been also reported in HCC. IFN induces apoptosis of human HCC cells (16), in case HCC cells are not resistant to apoptotic stimulation. Anti-apoptotic Bcl-2 family proteins may play an important role in this resistance (17,31,38,39). In this study, apoptosis was not induced and various aspects induced by IFN-α and sodium butyrate were confirmed not to be affected by apoptosis. *In vitro* studies demonstrated its anti-proliferative activity by inducing apoptosis or cell-cycle S-phase arrest. This cell-cycle arrest is considered to be due to p21/WAF1 induction and inhibition of cyclin A and B, which sequentially reduces cdk2 and cdc2 activities (30,40,41). Type I IFN was also demonstrated to inhibit angiogenesis of tumor vessels in nude mouse models (42,43). In addition, our previous studies demonstrated that IFN has an anti-metastasis effect by increasing cell-cell adhesion formed by E-cadherin and ß-catenin (25). Furthermore, telomerase activity was reduced and the present study demonstrated that IFN inhibits cancer cell invasion and metastasis by reducing MMP production of HCC cells. These observations confirm the

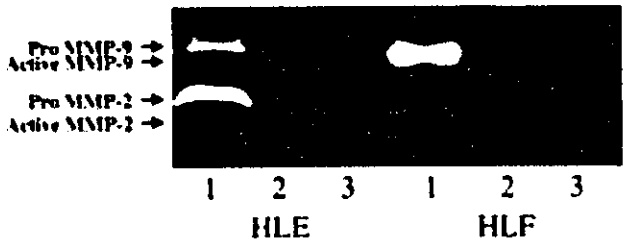

Figure 4. Gelatin zymography of the culture supernatants of HLE and HLF cells and the effect of IFN- and sodium butyrate-treatment. The serum-free culture supernatants of HLE and HLF with and without IFN and sodium butyrate for 7 days were collected. Equal amounts of protein were subjected to gelatin zymography described in Materials and methods. Destained band showed the existence of gelatinase. Control (lane 1), treated with 1000 IU/ml IFN-α (lane 2), treated with 2 mM SB (lane 3). Both HLE and HLF produced pro- and active MMP-2, and MMP-9. HLE produced MMP-2 much more than MMP-9, although HLF produced much more MMP-9 than MMP-2. The culture supernatants of HLE and HLF treated with IFN-α and sodium butyrate showed significant reduction of pro- and active-MMPs production in both cell lines. Especially MMP-2 activity almost disappeared in both cell lines. 1, Control; 2, IFN-α treatment (1000 IU/ml); 4, sodium butyrate treatment (2 mM).

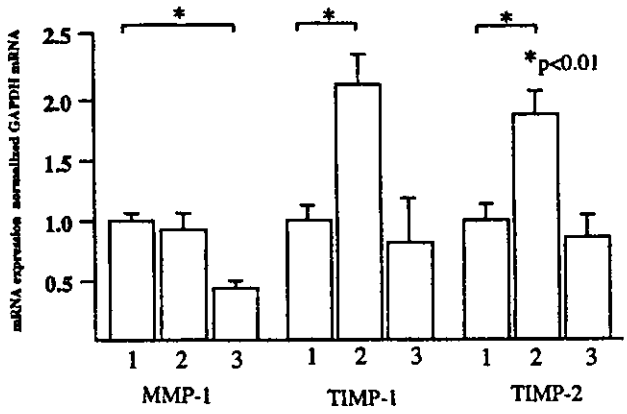

Figure 6. Real-time quantitative RT-PCR assay of MMP-1, TIMP-1 and TIPM-2. Effect of IFN-α and sodium butyrate on transcription of the MMP family and its counterpart, TIMP-1 and 2 of the HLE cell line was examined by real-time RT-PCR. The mRNA levels of MMP-1 decreased significantly by sodium butyrate. TIMP-1 and TIMP-2, which were counterparts of MMP-2, were significantly increased with treatment of 1000 U/ml of IFN-α ($p<0.01$, Mann Whitney's U test), although slightly decreased with treatment of 2 mM of sodium butyrate. Control (1), treated with 1000 IU/ml of IFN-α (2), treated with 2 mM of sodium butyrate (3).

theoretical background of recent clinical trials, which demonstrated that type I IFN was effective in advanced HCC (11,44) and inhibited secondary HCC raised after first treatment (45) other than acyclic retinoid (46,47). Recent studies have demonstrated that type I IFN directly activate p53 pathway not only in anti-viral but also in tumor suppression systems (48). We have demonstrated that interferon regulatory factor (IRF)-1 is a key transcription factor in the anti-proliferative activity of type I IFN (30), and it is possible that signal transduction of IFN depends on a type of single nucleotide polymorphisms in the IRF-1 promoter (18). Therefore anti-cancer effect of type I IFN on HCC may vary between individuals.

On the other hand, sodium butyrate is an HDAC inhibitor, which modifies histone acetylation and regulates gene expression (39). Recent studies revealed that a role of epigenetic conditions such as DNA methylation status and histone acetylation or methylation status are important factors in multistep carcinogenesis of human liver cancer especially that caused by chronic HCV infection. Hypomethylation in CpG islands of promoter regions in several oncogenes and deregulation of methylation enzymes have been demonstrated in human HCC (20,49,50). These epigenetic regulations of genomic expression are indispensable in human ontogeny or development and differentiation, suggesting that carcinogenesis and differentiation are closely related to each other. Sodium butyrate is categorized as one of differentiation inducers and its effects of increasing albumin production and decreasing α-fetoprotein production on HCC cells might be related to the cellular differentiation process.

MMP activity is considered to play an important role in invasion and metastasis activity of HCC. MMP-2 seems to be

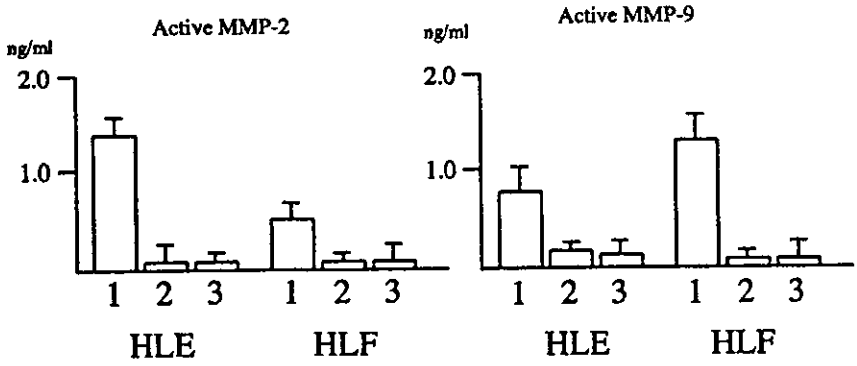

Figure 5. Quantitative analysis of active-form MMP-2 and -9 before and after treatment with IFN-α and sodium butyrate. The levels of active-type MMP-2 and -9 were assayed using the matrix metalloproteinase-2, -9 activity assay system. Control (1), treated with 1000 IU/ml of IFN-α (2), treated with 2 mM of sodium butyrate (3). Both active MMP-2 and MMP-9 levels produced by HLE cells were significantly decreased by IFN-α and sodium buytrate.

expressed in HCC especially in its peripheral region rather than central region of HCC, and the location is similar with that of MT1-MMP, which is an activator of MMP-2 (51), although negative data also exist (52). It seems true that the expression of active-form of MMP-2 is stronger in cancer than in non-cancer tissue in HCC (53,54). Active-forms of MMP-2 and -9 correlated with portal invasion, intrahepatic metastasis and recurrence rate after hepatic resection. MT1-MMP correlated with MMP-2 activation and invasion of HCC, and mRNA expression of this factor was positively shown in 22 cases in 30 HCCs. Ogata *et al* (54) demonstrated by immunostaining and *in situ* hybridization that expression of MT1-MMP and MMP-2 correlated to differentiation status of HCC tissues. Maatta *et al* (55) showed that MT1-MMP mRNA was expressed in HCC cells and its levels correlated to differentiation status of HCC, that is, the levels of expression is much more in poorly differentiated HCC than in well-differentiated type. MMP-2 expression levels of HCC may not be so different between cancer and the surrounding non-cancer tissue, but MMP-2 may be activated by MT1-MMP, which exists near the surrounding membrane of the tumor or membranous capsule, resulting in an increase of invasion potential (26). In addition, the balance of MMP-2 and TIMP-2 relates to metastasis potential (56). On the other hand, the localization of MMP-9 is closely correlated to tumor and malignant potential. Arii *et al* (52) showed that MMP-9 mRNA is detected only in the tumor, and its expression is higher in HCC with invasion through the membranous capsule. Immunostaining showed higher expression of this enzyme in the interface between tumor and non-tumor tissue. In the present study, both MMP-2 and MMP-9 expression and its activity was significantly reduced by IFN-α and sodium butyrate, suggesting that these two drugs are possibly useful for preventing HCC cells from invasion and metastasis.

Effect of IFN on MMP production or expression has been demonstrated in several types of cells. Type I IFN reduces MMP-2 production from glioma cells (57) and also reduces malignant potential of bladder cell carcinoma (58). These inhibitory effects of type I IFN on MMP production are induced via Stat-1 pathway in various types of cells (59,60). Another important mechanism may be a competitive binding of IRF-1 to NF-κB binding region in the MMP-9 promoter (61). It has been demonstrated that Stat-1, -2 and -3 are up-regulated by IFN-α in human HCC cell lines (62), and this pathway is responsible for up-regulation of MMP production.

In the present study, the effect of sodium butyrate, one of HDAC inhibitors, on HCC cells was similar with that of IFN-α, and our previous studies showed that effects of these two agents are very similar. It was demonstrated that Stat-1 expression is up-regulated in human HCC cell lines by sodium butyrate (63). This report suggests a possible crosstalk mechanism between sodium butyrate-induced and type I IFN-induced pathways. We investigated the gene expression after butyrate-stimulation in human HCC cells with a DNA micro-array, and one of the genes that increased by the stimulation was IRF-1, which is a key factor in the interferon system. This result also suggests that the reason why sodium butyrate shows a similar effect on HCC cells with IFN-α seems to be partially because of a crosstalk pathway between the effector systems in both agents. Other signal pathways may exist, because effects of these two agents on the expression of TIMP-1 and -2 were different from each other. Further investigation in these pathways may facilitate the development of a new therapeutic strategy.

Acknowlegments

We wish to thank Dr S. Houzawa (Tokai University, Japan) for kindly providing HT-1080 cells.

References

1. Nakamoto N, Saito H, Ebinuma H, Tada S, Saito Y, Kurita S, Kitamura K and Ishii H: Genomic mutations with amino acid substitutions of circulating hepatitis B virus found in non-B, non-C patients with hepatocellular carcinoma. Intern Med 42: 322-330, 2003.
2. Umeda T and Hino O: Molecular aspects of human hepatocarcinogenesis mediated by inflammation: from hypercarcinogenic state to normo- or hypocarcinogenic state. Oncology 62 (Suppl. 1): 38-42, 2002.
3. Poynard T, Bedossa P and Opolon P: Natural history of liver fibrosis progression in patients with chronic hepatitis C. The OBSVIRC, METAVIR, CLINIVIR, and DOSVIRC groups. Lancet 349: 825-832, 1997.
4. Arii S, Yamaoka Y, Futagawa S, Inoue K, Kobayashi K, Kojiro M, Makuuchi M, Nakamura Y, Okita K and Yamada R: Results of surgical and nonsurgical treatment for small-sized hepatocellular carcinomas: a retrospective and nationwide survey in Japan. The Liver Cancer Study Group of Japan. Hepatology 32: 1224-1229, 2000.
5. Yoshida H, Shiratori Y, Moriyama M, Arakawa Y, Ide T, Sata M, Inoue O, Yano M, Tanaka M, Fujiyama S, Nishiguchi S, Kuroki T, Imazeki F, Yokosuka O, Kinoyama S, Yamada G and Omata M: Interferon therapy reduces the risk for hepatocellular carcinoma: national surveillance program of cirrhotic and non-cirrhotic patients with chronic hepatitis C in Japan. IHIT Study Group. Inhibition of Hepatocarcinogenesis by Interferon Therapy. Ann Intern Med 131: 174-181, 1999.
6. Umeda T and Hino O: Hypercarcinogenic state in chronic liver disease. Intern Med 40: 555-556, 2001.
7. Curley SA: Radiofrequency ablation of malignant liver tumors. Ann Surg Oncol 10: 338-347, 2003.
8. Chander G, Sulkowski MS, Jenckes MW, Torbenson MS, Herlong HF, Bass EB and Gebo KA: Treatment of chronic hepatitis C: a systematic review. Hepatology 36: S135-S144, 2002.
9. Llovet JM and Bruix J: Systematic review of randomized trials for unresectable hepatocellular carcinoma: chemoembolization improves survival. Hepatology 37: 429-442, 2003.
10. Eguchi H, Nagano H, Yamamoto H, Miyamoto A, Kondo M, Dono K, Nakamori S, Umeshita K, Sakon M and Monden M: Augmentation of antitumor activity of 5-fluorouracil by interferon alpha is associated with up-regulation of p27Kip1 in human hepatocellular carcinoma cells. Clin Cancer Res 6: 2881-2890, 2000.
11. Miyamoto A, Umeshita K, Sakon M, Nagano H, Eguchi H, Kishimoto S, Dono K, Nakamori S, Gotoh M and Monden M: Advanced hepatocellular carcinoma with distant metastases, successfully treated by a combination therapy of alpha-interferon and oral tegafur/uracil. J Gastroenterol Hepatol 15: 1447-1451, 2000.
12. Miyaguchi S, Watanabe T, Takahashi H, Nakamura M, Saito H and Ishii H: Interferon therapy for hepatocellular carcinoma patients with low HCV-RNA levels. Hepatogastroenterology 49: 724-729, 2002.
13. Llovet JM, Sala M, Castells L, Suarez Y, Vilana R, Bianchi L, Ayuso C, Vargas V, Rodes J and Bruix J: Randomized controlled trial of interferon treatment for advanced hepatocellular carcinoma. Hepatology 31: 54-58, 2000.
14. Saito H, Kagawa T, Tada S, Tsunematsu S, Guevara FM, Watanabe T, Morizane T and Tsuchiya M: Effect of dexamethasone, dimethylsulfoxide and sodium butyrate on a human hepatoma cell line PLC/PRF/5. Cancer Biochem Biophys 13: 75-84, 1992.

15. Saito H, Morizane T, Watanabe T, Kagawa T, Miyaguchi S, Kumagai N and Tsuchiya M: Differentiating effect of sodium butyrate on human hepatoma cell lines PLC/PRF/5, HCC-M and HCC-T. Int J Cancer 48: 291-296, 1991.
16. Yano H, Iemura A, Haramaki M, Ogasawara S, Takayama A, Akiba J and Kojiro M: Interferon alfa receptor expression and growth inhibition by interferon alfa in human liver cancer cell lines. Hepatology 29: 1708-1717, 1999.
17. Saito H, Ebinuma H, Takahashi M, Kaneko F, Wakabayashi K, Nakamura M and Ishii H: Loss of butyrate-induced apoptosis in human hepatoma cell lines HCC-M and HCC-T having substantial Bcl-2 expression. Hepatology 27: 1233-1240, 1998.
18. Saito H, Tada S, Ebinuma H, Wakabayashi K, Takagi T, Saito Y, Nakamoto N, Kurita S and Ishii H: Interferon regulatory factor 1 promoter polymorphism and response to type 1 interferon. J Cell Biochem 81: 191-200, 2001.
19. Saito H, Tada S, Wakabayashi K, Nakamoto N, Takahashi M, Nakamura M, Ebinuma H and Ishii H: The detection of IRF-1 promoter polymorphisms and their possible contribution to T helper 1 response in chronic hepatitis C. J Interferon Cytokine Res 22: 693-700, 2002.
20. Saito Y, Kanai Y, Sakamoto M, Saito H, Ishii H and Hirohashi S: Expression of mRNA for DNA methyltransferases and methyl-CpG-binding proteins and DNA methylation status on CpG islands and pericentromeric satellite regions during human hepatocarcinogenesis. Hepatology 33: 561-568, 2001.
21. Tsutsumi T, Ido A, Nakao K, Hamasaki K, Kato Y, Ohtsuru A, Nakata K, Tamaoki T and Nagataki S: Reciprocal regulation of alpha-fetoprotein and albumin gene expression by butyrate in human hepatoma cells. Gastroenterology 107: 499-504, 1994.
22. Ebinuma H, Saito H, Saito Y, Wakabayashi K, Nakamura M, Kurose I and Ishii H: Antisense oligodeoxynucleotide against c-myc mRNA induces differentiation of human hepatocellular carcinoma cells. Int J Oncol 15: 991-999, 1999.
23. Ebinuma H, Saito H, Kosuga M, Wakabayashi K, Saito Y, Takagi T, Nakamoto N, Okuyama T and Ishii H: Reduction of c-myc expression by an antisense approach under Cre/loxP switching induces apoptosis in human liver cancer cells. J Cell Physiol 188: 56-66, 2001.
24. Nakamura M, Saito H, Ebinuma H, Wakabayashi K, Saito Y, Takagi T, Nakamoto N and Ishii H: Reduction of telomerase activity in human liver cancer cells by a histone deacetylase inhibitor. J Cell Physiol 187: 392-401, 2001.
25. Masuda T, Saito H, Kaneko F, Atsukawa K, Morita M, Inagaki H, Kumagai N, Tsuchimoto K and Ishii AH: Up-regulation of E-cadherin and ß-catenin in human hepatocellular carcinoma cell lines by sodium butyrate and interferon-alpha. In Vitro Cell Dev Biol Anim 36: 387-394, 2000.
26. Giannelli G, Bergamini C, Fransvea E, Marinosci F, Quaranta V and Antonaci S: Human hepatocellular carcinoma (HCC) cells require both alpha3beta1 integrin and matrix metalloproteinases activity for migration and invasion. Lab Invest 81: 613-627, 2001.
27. Dor I, Namba M and Sato J: Establishment and some biological characteristics of human hepatoma cell lines. Gann 66: 385-392, 1975.
28. Saito H, Morizane T, Watanabe T, Kagawa T, Iwabuchi MN, Kumagai N, Inagaki Y, Tsuchimoto K and Tsuchiya M: Establishment of a human cell line (HCC-T) from a patient with hepatoma bearing no evidence of hepatitis B or A virus infection. Cancer 64: 1054-1060, 1989.
29. Watanabe T, Morizane T, Tsuchimoto K, Inagaki Y, Munakata Y, Nakamura T, Kumagai N and Tsuchiya M: Establishment of a cell line (HCC-M) from a human hepatocellular carcinoma. Int J Cancer 32: 141-146, 1983.
30. Tada S, Saito H, Tsunematsu S, Ebinuma H, Wakabayashi K, Masuda T and Ishii H: Interferon regulatory factor-1 gene abnormality and loss of growth inhibitory effect of interferon-alpha in human hepatoma cell lines. Int J Oncol 13: 1207-1216, 1998.
31. Takahashi M, Saito H, Okuyama T, Miyashita T, Kosuga M, Sumisa F, Yamada M, Ebinuma H and Ishii H: Overexpression of Bcl-2 protects human hepatoma cells from Fas-antibody-mediated apoptosis. J Hepatol 31: 315-322, 1999.
32. Chung TW, Moon SK, Lee YC, Kim JG, Ko JH and Kim CH: Enhanced expression of matrix metalloproteinase-9 by hepatitis B virus infection in liver cells. Arch Biochem Biophys 408: 147-154, 2002.
33. Nomura H, Fujimoto N, Seiki M, Mai M and Okada Y: Enhanced production of matrix metalloproteinases and activation of matrix metalloproteinase 2 (gelatinase A) in human gastric carcinomas. Int J Cancer 69: 9-16, 1996.
34. Verheijen JH, Nieuwenbroek NM, Beekman B, Hanemaaijer R, Verspaget HW, Ronday HK and Bakker AH: Modified proenzymes as artificial substrates for proteolytic enzymes: colorimetric assay of bacterial collagenase and matrix metalloproteinase activity using modified pro-urokinase. Biochem J 323: 603-609, 1997.
35. Kohyama T, Liu X, Zhu YK, Wen FQ, Wang HJ, Fang Q, Kobayashi T and Rennard SI: Phosphodiesterase 4 inhibitor cilomilast inhibits fibroblast-mediated collagen gel degradation induced by tumor necrosis factor-alpha and neutrophil elastase. Am J Respir Cell Mol Biol 27: 487-494, 2002.
36. Sun HB and Yokota H: Reduction of cytokine-induced expression and activity of MMP-1 and MMP-13 by mechanical strain in MH7A rheumatoid synovial cells. Matrix Biol 21: 263-270, 2002.
37. Bogdan C: The function of type I interferons in antimicrobial immunity. Curr Opin Immunol 12: 419-424, 2000.
38. Takahashi M, Saito H, Atsukawa K, Ebinuma H, Okuyama T and Ishii H: Bcl-2 prevents doxorubicin-induced apoptosis of human liver cancer cells. Hepatol Res 25: 192-201, 2003.
39. Wakabayashi K, Saito H, Ebinuma H, Saito Y, Takagi T, Nakamura M, Umezawa A, Hata J and Ishii H: Bcl-2 related proteins are dramatically induced at the early stage of differentiation in human liver cancer cells by a histone deacetylase inhibitor projecting an anti-apoptotic role during this period. Oncol Rep 7: 285-288, 2000.
40. Detjen KM, Welzel M, Farwig K, Brembeck FH, Kaiser A, Riecken EO, Wiedenmann B and Rosewicz S: Molecular mechanism of interferon alfa-mediated growth inhibition in human neuroendocrine tumor cells. Gastroenterology 118: 735-748, 2000.
41. Murphy D, Detjen KM, Welzel M, Wiedenmann B and Rosewicz S: Interferon-alpha delays S-phase progression in human hepatocellular carcinoma cells via inhibition of specific cyclin-dependent kinases. Hepatology 33: 346-356, 2001.
42. Wang L, Tang ZY, Qin LX, Wu XF, Sun HC, Xue Q and Ye SL: High-dose and long-term therapy with interferon-alfa inhibits tumor growth and recurrence in nude mice bearing human hepatocellular carcinoma xenografts with high metastatic potential. Hepatology 32: 43-48, 2000.
43. Wang L, Wu WZ, Sun HC, Wu XF, Qin LX, Liu YK, Liu KD and Tang ZY: Mechanism of interferon alpha on inhibition of metastasis and angiogenesis of hepatocellular carcinoma after curative resection in nude mice. J Gastrointest Surg 7: 587-594, 2003.
44. Lai CL, Lau JY, Wu PC, Ngan H, Chung HT, Mitchell SJ, Corbett TJ, Chow AW and Lin HJ: Recombinant interferon-alpha in inoperable hepatocellular carcinoma: a randomized controlled trial. Hepatology 17: 389-394, 1993.
45. Ikeda K, Arase Y, Saitoh S, Kobayashi M, Suzuki Y, Suzuki F, Tsubota A, Chayama K, Murashima N and Kumada H: Interferon beta prevents recurrence of hepatocellular carcinoma after complete resection or ablation of the primary tumor-A prospective randomized study of hepatitis C virus-related liver cancer. Hepatology 32: 228-332, 2000.
46. Muto Y, Moriwaki H, Ninomiya M, Adachi S, Saito A, Takasaki KT, Tanaka T, Tsurumi K, Okuno M, Tomita E, Nakamura T and Kojima T: Prevention of second primary tumors by an acyclic retinoid, polyprenoic acid, in patients with hepatocellular carcinoma. Hepatoma Prevention Study Group. N Engl J Med 334: 1561-1567, 1996.
47. Muto Y, Moriwaki H and Saito A: Prevention of second primary tumors by an acyclic retinoid in patients with hepatocellular carcinoma. N Engl J Med 340: 1046-1047, 1999.
48. Takaoka A, Hayakawa S, Yanai H, Stoiber D, Negishi H, Kikuchi H, Sasaki S, Imai K, Shibue T, Honda K and Taniguchi T: Integration of interferon-alpha/beta signalling to p53 responses in tumour suppression and antiviral defence. Nature 424: 516-523, 2003.
49. Saito Y, Kanai Y, Sakamoto M, Saito H, Ishii H and Hirohashi S: Overexpression of a splice variant of DNA methyltransferase 3b, DNMT3b4, associated with DNA hypomethylation on peri-centromeric satellite regions during human hepatocarcinogenesis. Proc Natl Acad Sci USA 99: 10060-10065, 2002.

50. Saito Y, Kanai Y, Nakagawa T, Sakamoto M, Saito H, Ishii H and Hirohashi S: Increased protein expression of DNA methyltransferase (DNMT) 1 is significantly correlated with the malignant potential and poor prognosis of human hepatocellular carcinomas. Int J Cancer 105: 527-532, 2003.
51. Harada T, Arii S, Mise M, Imamura T, Higashitsuji H, Furutani M, Niwano M, Ishigami S, Fukumoto M, Seiki M, Sato H and Imamura M: Membrane-type matrix metalloproteinase-1(MT1-MTP) gene is overexpressed in highly invasive hepatocellular carcinomas. J Hepatol 28: 231-239, 1998.
52. Arii S, Mise M, Harada T, Furutani M, Ishigami S, Niwano M, Mizumoto M, Fukumoto M and Imamura M: Overexpression of matrix metalloproteinase 9 gene in hepatocellular carcinoma with invasive potential. Hepatology 24: 316-322, 1996.
53. Yamamoto H, Itoh F, Adachi Y, Sakamoto H, Adachi M, Hinoda Y and Imai K: Relation of enhanced secretion of active matrix metalloproteinases with tumor spread in human hepatocellular carcinoma. Gastroenterology 112: 1290-1296, 1997.
54. Ogata R, Torimura T, Kin M, Ueno T, Tateishi Y, Kuromatsu R, Shimauchi Y, Sakamoto M, Tamaki S, Sata M and Tanikawa K: Increased expression of membrane type 1 matrix metalloproteinase and matrix metalloproteinase-2 with tumor dedifferentiation in hepatocellular carcinomas. Hum Pathol 30: 443-450, 1999.
55. Maatta M, Soini Y, Liakka A and Autio-Harmainen H: Differential expression of matrix metalloproteinase (MMP)-2, MMP-9, and membrane type 1-MMP in hepatocellular and pancreatic adenocarcinoma: implications for tumor progression and clinical prognosis. Clin Cancer Res 6: 2726-2734, 2000.
56. Giannelli G, Bergamini C, Marinosci F, Fransvea E, Quaranta M, Lupo L, Schiraldi O and Antonaci S: Clinical role of MMP-2/TIMP-2 imbalance in hepatocellular carcinoma. Int J Cancer 97: 425-431, 2002.
57. Wiranowska M, Rojiani AM, Gottschall PE, Moscinski LC, Johnson J and Saporta S: CD44 expression and MMP-2 secretion by mouse glioma cells: effect of interferon and anti-CD44 antibody. Anticancer Res 20: 4301-4306, 2000.
58. Slaton JW, Karashima T, Perrotte P, Inoue K, Kim SJ, Izawa J, Kedar D, McConkey DJ, Millikan R, Sweeney P, Yoshikawa C, Shuin T and Dinney CP: Treatment with low-dose interferon-alpha restores the balance between matrix metalloproteinase-9 and E-cadherin expression in human transitional cell carcinoma of the bladder. Clin Cancer Res 7: 2840-2853, 2001.
59. Ma Z, Qin H and Benveniste EN: Transcriptional suppression of matrix metalloproteinase-9 gene expression by IFN-gamma and IFN-beta: critical role of STAT-1alpha. J Immunol 167: 5150-5159, 2001.
60. Huang S, Bucana CD, van Arsdall M and Fidler IJ: Stat1 negatively regulates angiogenesis, tumorigenicity and metastasis of tumor cells. Oncogene 21: 2504-2512, 2002.
61. Sanceau J, Boyd DD, Seiki M and Bauvois B: Interferons inhibit tumor necrosis factor-alpha-mediated matrix metalloproteinase-9 activation via interferon regulatory factor-1 binding competition with NF-kappa B. J Biol Chem 277: 35766-35775, 2002.
62. Radaeva S, Jaruga B, Hong F, Kim WH, Fan S, Cai H, Strom S, Liu Y, El-Assal O and Gao B: Interferon-alpha activates multiple STAT signals and down-regulates c-Met in primary human hepatocytes. Gastroenterology 122: 1020-1034, 2002.
63. Hung WC and Chuang LY: Sodium butyrate enhances STAT 1 expression in PLC/PRF/5 hepatoma cells and augments their responsiveness to interferon-alpha. Br J Cancer 80: 705-710, 1999.

Journal of Viral Hepatitis, 2004, 11, 225–235

Polymorphisms of NS5B protein relates to early clearance of hepatitis C virus by interferon plus ribavirin: a pilot study

N. Kumagai,[1] N. Takahashi,[2] M. Kinoshita,[2] S. Tsunematsu,[1] K. Tsuchimoto,[1] H. Saito[3] and H. Ishii[3] [1]*Research Center for Liver Diseases, the Kitasato Institute, Minato-ku, Tokyo, Japan;* [2]*Gene Analysis Center, Otsuka Life Science Initiative, Otsuka Pharmaceutical Co. Ltd., Kawauchi-cho, Tokushima, Japan; and* [3]*Department of Internal Medicine, School of Medicine, Keio University, Shinjuku-ku, Tokyo, Japan*

Received in revised form October 2003; accepted for publication November 2003

SUMMARY. Although randomized trials have shown enhancement of efficacy for combination therapy with interferon (IFN) α-2b and ribavirin compared with IFN monotherapy as first-line treatment for chronic hepatitis C, infection with genotype 1b and high viremia are still associated with significantly low response rates compared with non-1 genotypes and low viremia. We analysed amino acid sequences of the viral RNA-dependent RNA polymerase (RdRP) or nonstructural protein 5B (NS5B), responsible for ribavirin misincorporation into RNA products in patients with genotype 1b-related chronic hepatitis C and high viremia, and examined the relationship between such RdRp polymorphisms, and the initial decline in viral load induced by combination therapy with IFN-α and ribavirin. Substitution of glutamic acid to lysine at the 124th position (E124K) and of isoleucine to valine at the 85th position (I85V) were found to be closely associated with a potent decline of viral load and viral clearance at 8 weeks of treatment (five of five patients, coincidence rate 100%). In conclusion, our results suggest that the polymorphisms of E124K and I85V identified in NS5B protein are crucial for early viral clearance in patients with genotype 1b and high viremia by combination therapy with IFN and ribavirin, and that detection of amino acid sequence motifs might enable prediction of clinical efficacy.

Keywords: amino acid sequence motifs, direct sequencing, genotype 1b, hepatitis C virus, nucleoside analogue, RNA-dependent RNA polymerase.

INTRODUCTION

Chronic infection with hepatitis C virus (HCV) is a common cause of chronic hepatitis, which in many patients progresses to cirrhosis and hepatocellular carcinoma. Until recently, interferon-alpha (IFN-α) and interferon-beta (IFN-β) were the only available treatments for HCV infection in Japan, although only 10–15% of treated subjects achieved sustained viral eradication. Ribavirin, a nucleoside analogue, exhibits *in vitro* activity against some DNA and RNA viruses, including certain members of *Flaviviridae*. Although ribavirin cannot decrease serum HCV RNA level in patients by itself, it has been demonstrated that combination therapy with IFN-α and ribavirin yields a higher sustained response rate than IFN-α monotherapy [1–3]. Moreover, the recently developed pegylated IFN and ribavirin combination therapy is more effective for chronic hepatitis C patients, although half of patients with HCV genotype 1b and high baseline levels of viral RNA do not achieve sustained virological response with it [4,5].

Ribavirin is a broad-spectrum antiviral nucleoside analogue that is converted to mono-, di- and triphosphorylated forms inside of cells. It has recently been demonstrated that the antiviral activity of ribavirin can result from the ability of a viral RNA-dependent RNA polymerase (RdRP) to utilize ribavirin triphosphate and to incorporate this nucleotide into the viral genome with reduced specificity, thereby mutagenizing the genome and decreasing the yield of infectious virus [6]. Moreover, ribavirin exhibits an antiviral effect through a mechanism of error-prone replication in the HCV subgenomic replication system [7].

In genotype 1b-infected patients, a potent antiviral effect on HCV viral dynamics in serum during combination therapy with IFN-α and ribavirin has been reported. The initial decline in viral load predicts the outcome of therapy: sustained virological responders have either an undetectable plasma HCV RNA level at day 14 [8] or >99.9% decrease of viral load within 4 weeks [9].

Abbreviations: HCV, hepatitis C virus; IFN, interferon; PCR, polymerase chain reaction; RdRP, RNA-dependent RNA polymerase; RT, reverse transcription.

Correspondence: Naoki Kumagai MD, Research Center for Liver Diseases, the Kitasato Institute, 5-9-1 Shirokane, Minato-ku, Tokyo 108-8642, Japan. E-mail: kumagai-n@kitasato.or.jp

In this study, we analysed amino acid sequences of RdRP (NS5B) in patients with genotype 1b-related chronic hepatitis C and examined the relationship of polymorphisms of RdRP and the degree of initial decline in viral load during combination therapy with IFN-α and ribavirin. We identified the amino acid sequence motifs of RdRP that were highly correlated with early clearance of HCV.

PATIENTS AND METHODS

Patients

Eight patients with chronic hepatitis C associated with genotype 1b with high viral load (>500 KIU/mL by Amplicor-HCV monitor ver. 2.0 assay; Roche Molecular Diagnostics Co., Tokyo, Japan) were included in the present study. Two patients had previously been treated with IFN-α alone and six patients had not previously taken IFN. Written informed consent was obtained from all patients, and the protocol of the present study was approved by the local ethics committee of Kitasato Institute Hospital.

Treatment schedule

All patients received 10 MIU IFN-α 2b (Intron A®, Schering-Plough, K.K., Osaka, Japan)/day for 2 weeks followed by 6 MIU t.i.w. of IFN-α 2b for 22 weeks. During the treatment, all patients received the same amount of ribavirin: 600 mg/day (<60 kg body weight) or 800 mg/day (>60 kg). Adjustment of therapy was performed according to changes in haemoglobin, WBC, and platelet count using standard criteria for IFN/ribavirin combination therapy, although no patients exhibited change in amount of ribavirin during the first 8 weeks of therapy.

Measurement of serum ribavirin concentrations

In order to ascertain steady administration of ribavirin in patients, we measured the ribavirin concentration in serum using a solid-phase extraction, high-performance liquid chromatography assay [10] after 8 weeks of administration, when the concentration is generally believed to have reached a plateau [11].

Table 1 Sequences of oligonucleotide primers and their locations in the HCV-RNA genome

Primers	Sequences (5′ to 3′)	Length (base)	Sense	Nucleotide positions*
HCV-1b-7481F	5′-ATGCCCCCCCTYGAGGGRGARCCRGGGGACCC-3′	30	+	7481–7512
HCV-1b-9396R	5′-ATGGCCTATTGGCCTGGAGTG-3′	21	−	9377–9396
HCV-1b-7527F	5′-CTCAGYGACGGGTCTTGGTCTACCGTGAGC-3′	30	+	7527–7556
HCV-1b-9374R	5′-TTAKCTCCCCGYTCAYCGRTTGGGGAGC-3′	28	−	9347–9374
HCV-1b-7947F	5′-TCCGTGTGGRAGGACYTGCTGGARGACACT-3′	30	+	7947–7976
HCV-1b-8397F	5′-GGGCAGARCTGYGGTTATCGCCGGTGCCGC-3′	30	+	8397–8426
HCV-1b-8878R	5′-GAGAAGAARTGRGTCATCARAATCAT-3′	26	−	8853–8878

*Coordinates refer to nucleotide position in the HCV-J strain (accession No. D90208).
In the primer sequences, Y denotes T or C, R denotes A or G and K denotes G or T.

Table 2 Baseline characteristics and HCV-RNA level at 8 weeks of treatment with IFN in combination with ribavirin

Patient No., gender/age	Histological diagnosis	Previous IFN therapy (yes /no)	Baseline ALT level (IU/L)	Baseline HCV RNA (KIU/mL)	Serum ribavirin at 8 weeks Tx (ng/mL)	HCV RNA at 8 weeks Tx (KIU/mL)
1 F/65	CAH	No	156	850<	3089	–
2 M/51	CAH	No	145	690	2152	–
3 M/55	CAH	Yes	210	850<	4216	–
4 M/51	CAH	No	46	850<	2632	–
5 M/65	CAH	No	58	850<	2901	–
6 F/53	CAH	No	118	850<	1800	260
7 M/55	CAH	Yes	232	520	2922	330
8 M/53	CAH	No	80	830	1598	320

*CAH, chronic active hepatitis; HCV, hepatitis C virus; IFN, interferon; ALT, alanine aminotransferase; Tx, treatment.

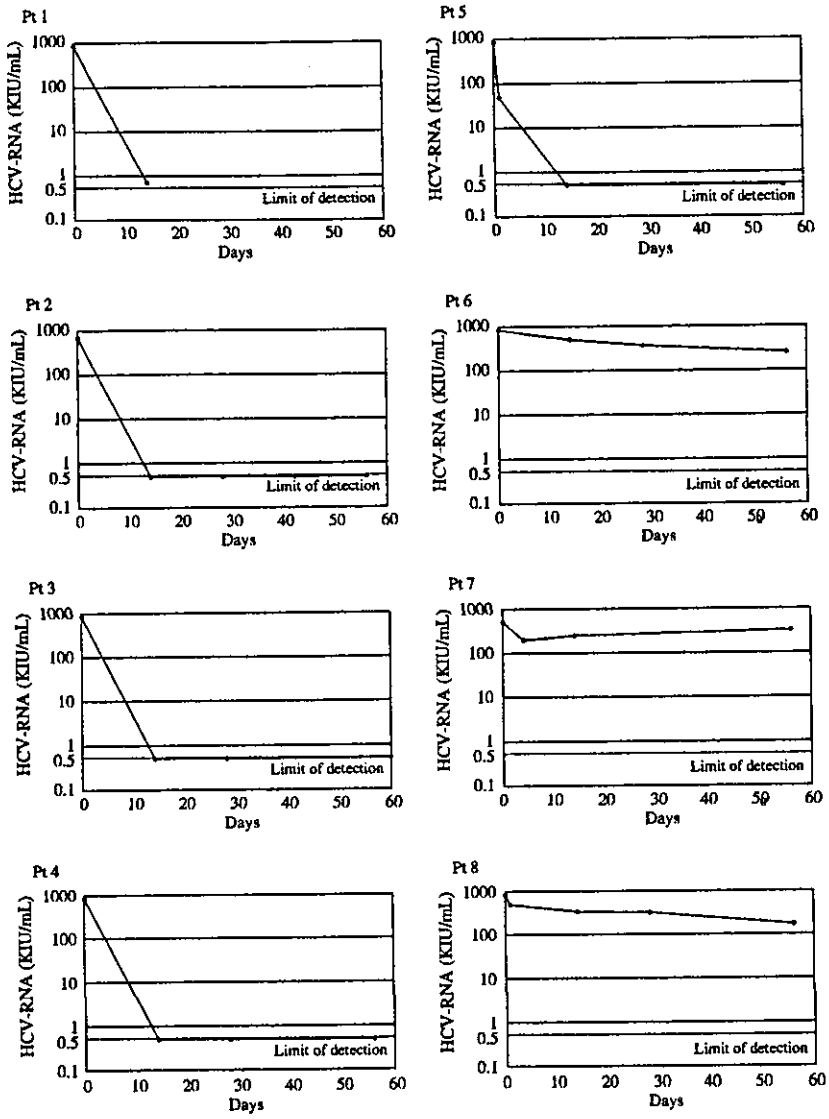

Fig. 1 Viral load in serum during the first 8 weeks of combination therapy with IFN and ribavirin for eight patients (pt 1 to pt 8) infected with HCV genotype 1b with high initial viral load.

Determination of viral load of HCV RNA in serum

Blood was obtained from the patients on day 0, (before administration of IFN) and days 1, 14, 28, and 56 of treatment. Total RNA was extracted from serum, and HCV RNA in serum at each time point was quantified by Amplicor® HCV monitor ver. 2.0 assay.

Primers for RdRP amplification

The primer sequences used for this study are shown in Table 1. These primers were obtained with an ABI-394 DNA synthesizer (Applied Biosystems Inc., Foster City, CA, USA) using a protocol described previously [12]. Outer primers HCV-1b-7481F [13] and HCV-1b-9396R, and inner primers HCV-1b-7527F, and HCV-1b-9374R, were used for nested polymerase chain reaction (PCR). Primers HCV-1b-7947F, HCV-1b-8397F and HCV-1b-8878R were used for sequencing reactions.

Direct sequencing of the NS5B region coding RdRP of HCV RNA

HCV RNA was isolated from a 100 μL aliquot of each serum sample by the Acid Guanidium-Phenol-Chloroform method described previously [14]. Obtained RNA was reverse-transcribed to complementary DNA (cDNA) using SuperScript 2 reverse-transcriptase (Invitrogen Corp., Carlsbad, CA, USA) with random primers. The resulting cDNA was amplified by PCR using primers HCV-1b-7481F and HCV-1b-9396R and the Takara LA Taq DNA polymerase (Takara Shuzo, Otsu, Japan) in a 9600 GeneAmp® PCR System (Applied Biosystems Inc.). PCR was performed for 40 cycles. Each PCR reaction cycle included denaturation at 94 °C for 30 s,

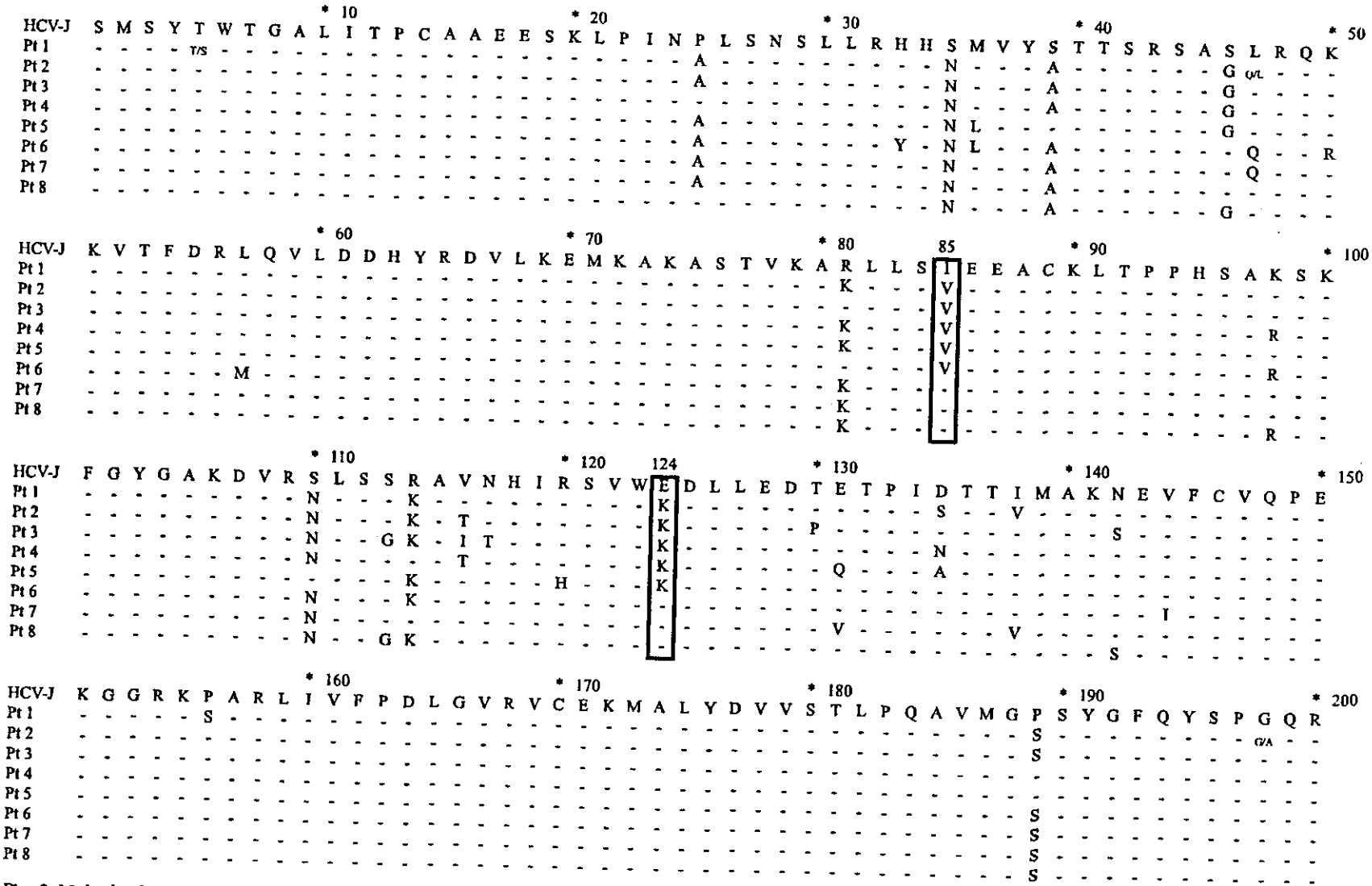

Fig. 2 Multiple alignment of HCV NS5B amino acid sequences. Sample sequences are shown of the first 577 residues of HCV NS5B compared with the HCV-J strain (accession: GNWVCJ). Amino acid residues at the 85 and 124th position are indicated in boxes.

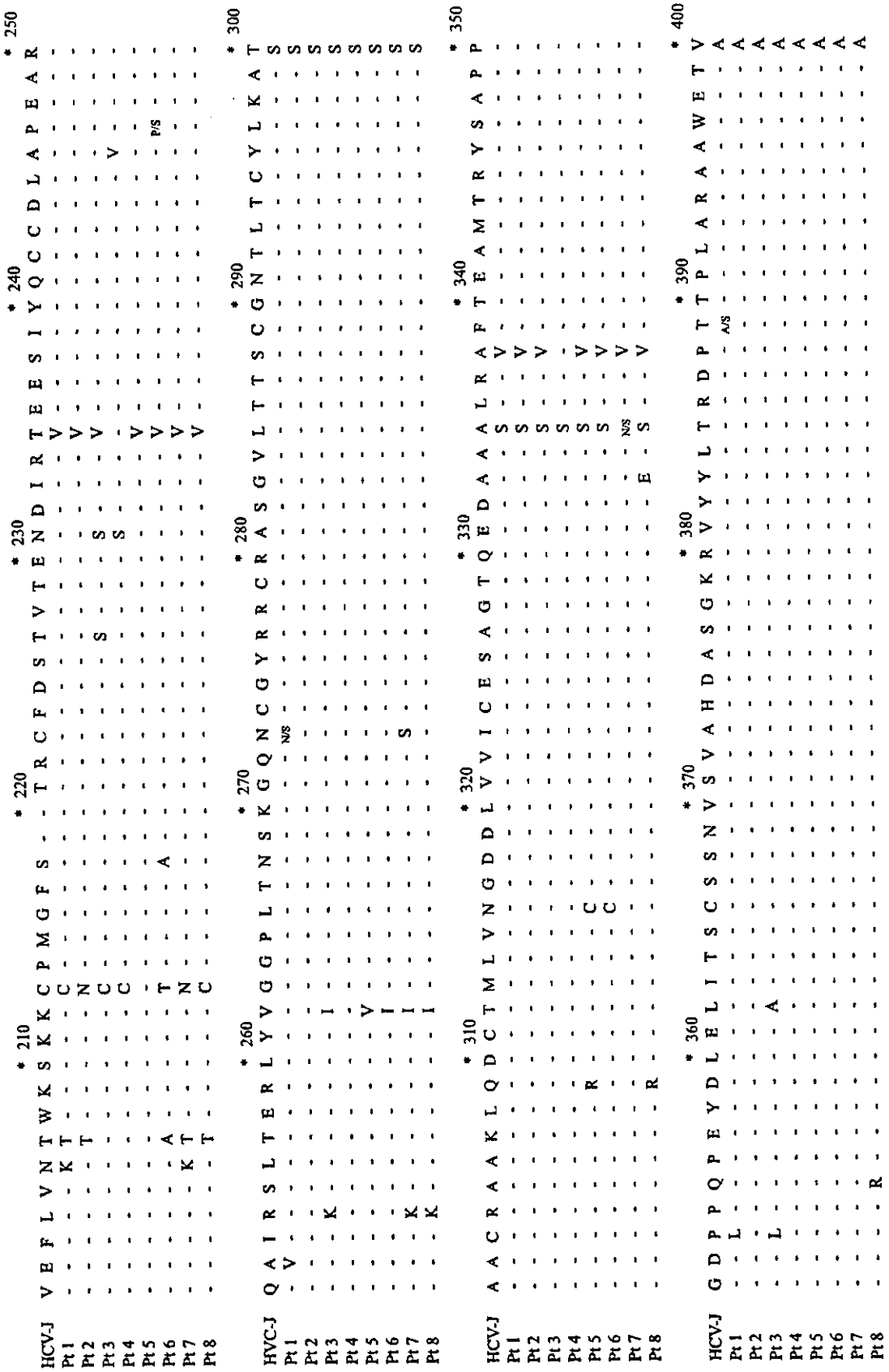

Fig. 2 (*Contd.*)

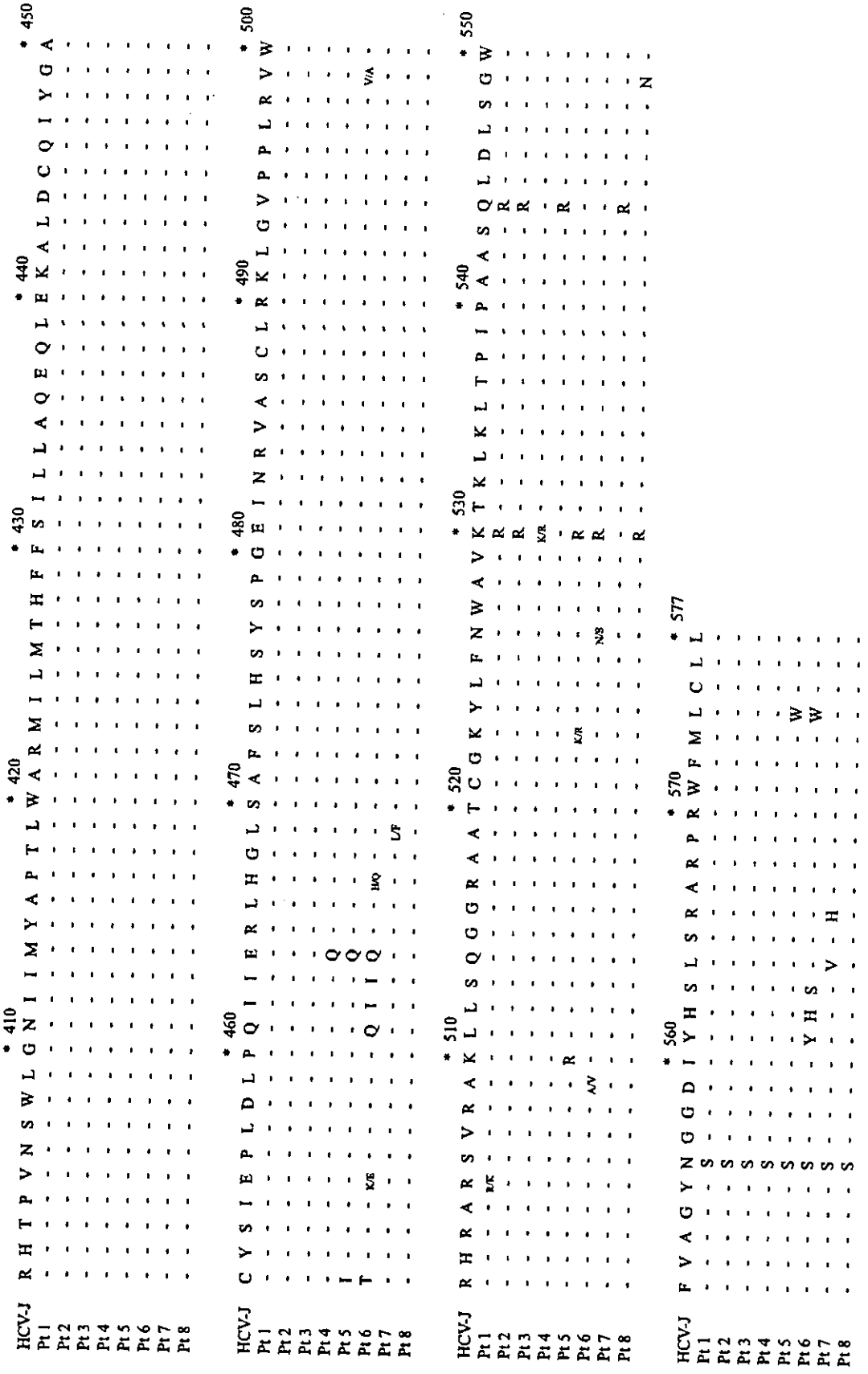
HCV-J R H T P V N S W L G N I I M Y A P T L W A R M I L M T H F F S I L L A Q E Q L E K A L D C Q I Y G A
Pt 1
Pt 2
Pt 3
Pt 4
Pt 5
Pt 6
Pt 7
Pt 8
HCV-J C Y S I E P L D L P Q I I E R L H G L S A F S L H S Y S P G E I N R V A S C L R K L G V P P L R V W
Pt 1
Pt 2
Pt 3
Pt 4
Pt 5
Pt 6
Pt 7
Pt 8
HCV-J R H R A R S V R A K L L S Q G G R A A T C G K Y L F N W A V K T K L K L T P I P A A S Q L D L S G W
Pt 1
Pt 2
Pt 3
Pt 4
Pt 5
Pt 6
Pt 7
Pt 8
HCV-J F V A G Y N G G D I Y H S L S R A R P R W F M L C L L
Pt 1
Pt 2
Pt 3
Pt 4
Pt 5
Pt 6
Pt 7
Pt 8

Fig. 2 (*Contd.*)

Table 3 Amino acid residues at positions 85 and 124, and viral clearance

Patient No.	Initial decrease in serum HCV RNA*	Viral clearance in serum at 8 weeks Tx	NS5B	
			Position 85	Position 124
1	3.1 log	Yes	V	K
2	3.1 log	Yes	V	K
3	3.2 log	Yes	V	K
4	3.2 log	Yes	V	K
5	3.2 log	Yes	V	K
6	0.2 log	No	I	E
7	−0.1 log	No	I	E
8	0.4 log	No	I	E

*Initial decrease showed in 2 weeks after administration.

primer annealing at 60 °C for 30 s, and primer extension at 72 °C for 120 s. Nested PCR was performed with 2 μL of the first PCR-products under the same conditions as for the first round. We then separated the nested PCR-products by 1.0% agarose gel electrophoresis and purified the 1848 bp-long amplicons. Purified fragments were subjected to cycle sequencing using the primers in Table 1, and excess dNTPs were removed with gel filtration using Sephadex G-50 (Pharmacia Biotech). Direct sequence comparisons were performed using the ABI PRISM 3100 Genetic Analyzer (Applied Biosystems Inc.).

Protein structure prediction

A tertiary structure model of HCV RdRp protein from patients was generated by SWISS-MODEL, and ribbon models and molecular surfaces with electrostatic potential were illustrated with a Swiss-Plot Database Viewer [15]. The SWISS-MODEL program automatically finds all similarities in the target sequence with sequences of known structure using the BLASTP2 program, and generates tertiary models with the ProMod II program. Energy minimizations of the models were then calculated using the GROMOS96 program. The models of HCV RdRp from patients in this study were built using HCV RdRp X-ray structures deposited in the Protein Data Bank as templates (Protein Data Bank numbers 1C2PB, 1C2PA, 1QUVA, 1GX5A, 1CSJB, 1CSJA, 1GX6A). In the reported models, most of the residues were in the most favoured region of the Ramachandran plot (96.5%). Crystal structure models of HCV RdRp for HCV-BK (Protein Data Bank number 1QUV) and HC-J4 (Protein Data Bank number 1NB6) were used for reference.

RESULTS

The demographic, clinical, histological, and virological characteristics and clinical outcome of combination therapy with IFN and ribavirin for the eight patients are shown in Table 2. Patients in whom HCV RNA could not be detected after 8 weeks of treatment were defined as 'good responders', while patients in whom HCV RNA remained detectable after 8 weeks treatment were defined as poor responders. Patients 1–5 were good responders and patients 6–8 were poor responders. Hepatitis C viral dynamics in serum for the eight patients during therapy are shown in Fig. 1.

Amplicons of the NS5B region of HCV RNA from these patients were directly sequenced, and the nucleic acid sequences were compared phylogenetic tree analysis. However, no clusters that discriminated between good and poor responders were observed. We then searched for a single mutation that may have been responsible for viral clearance. Figure 2 shows a multiple alignment of amino acid sequences of the NS5B region of HCV compared with the HCV-J strain [13], which is generally considered IFN- resistant. We noticed that substitution of glutamic acid at the 124th position by lysine yielded a complete match with the population of good responders (five of five). Substitution of isoleucine at the 85th position by valine also appeared relevant to viral clearance (five of five) (Table 3). These positions of nucleic acid substitution were identical in each patient, although quasispecies were observed.

DISCUSSION

Combined use of IFN-α and ribavirin has become first-line treatment for patients with chronic hepatitis C since 2000 [1,2]. The efficacy of pegylated IFN-α 2a or −α 2b plus ribavirin has recently been reported [16,17]. Although ribavirin enhanced the efficacy of interferon in patients with hepatitis C, the viral eradication rate is still low in patients infected with genotype 1b of HCV [1,18]. Disappearance of serum HCV RNA as measured by PCR after 12–24 weeks of treatment is useful for predicting sustained viral response, as are genotype and baseline viral load, stage of fibrosis, gender, and age. Thus, disappearance of HCV-RNA in serum during the early stage of treatment is necessary for sustained viral response [19]. In a study of serum HCV dynamics, the exponential decay slopes calculated from the second phase of

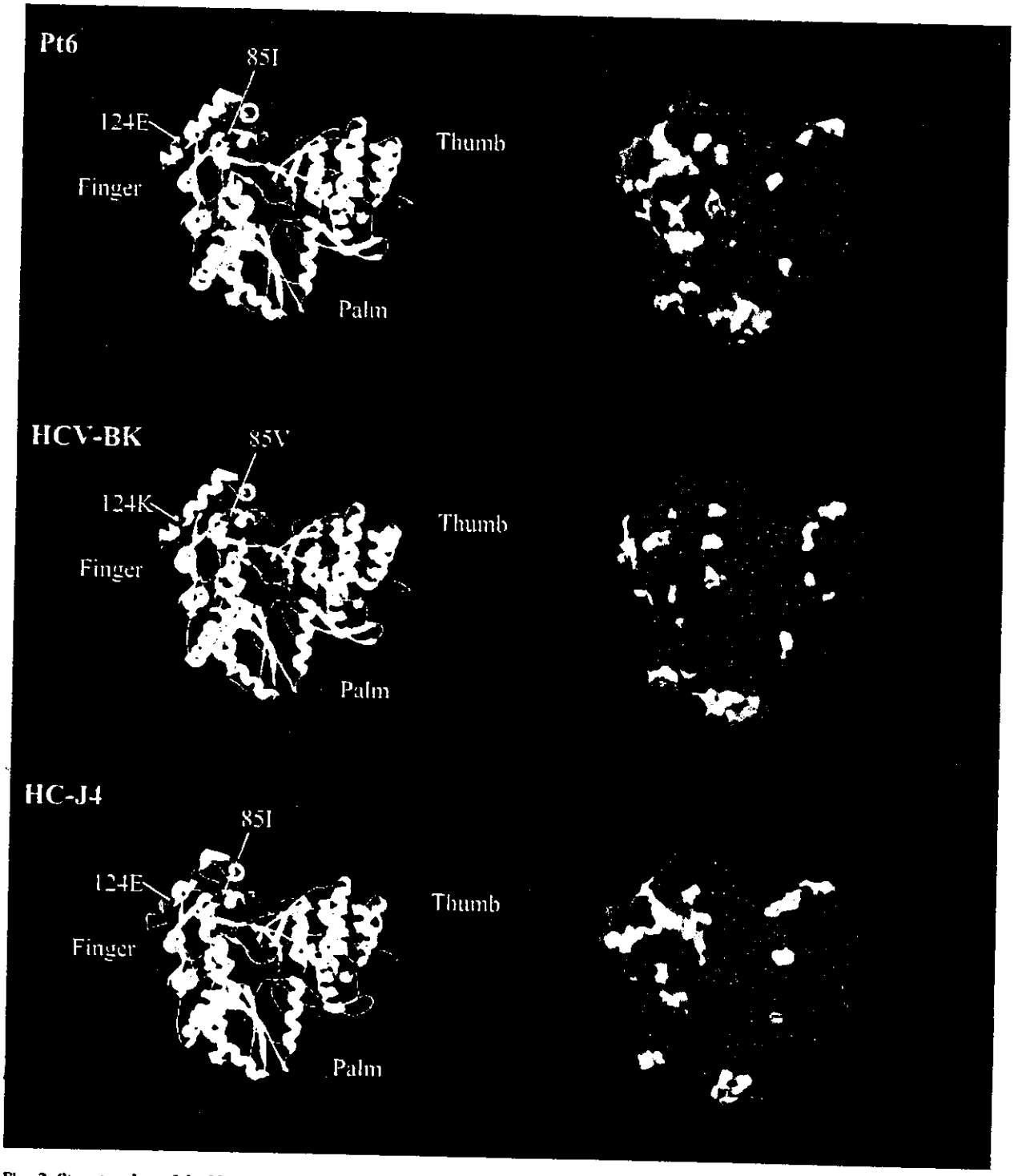

Fig. 3 Structural model of hepatitis C virus RNA-dependent RNA polymerase (NS5B). The structure of the HCV NS5B from patient 6 was predicted with the SWISS-MODEL program (15). Ribbon diagrams (left panel) and molecular surfaces with electrostatic potential (right panel) were obtained with the Swiss-Plot Database Viewer (15). In the ribbon diagrams, positions of isoleucine 85 and glutamic acid 124 are represented in red. Each of the upper panels shows HCV NS5B from Pt 6, which has isoleucine at the 85th position and glutamic acid at the 124th position, and each of the middle panels shows HCV NS5B of the HCV-BK strain (1QUV) (28), which has valine at the 85th position and lysine at the 124th position. Each of the bottom panels shows HCV NS5B of HC-J4 strain (1NB7)(29), which has valine at the 85th position and lysine at the 124th position. In surface models with electrostatic potential, positive and negative charges are indicated in blue and red, respectively.

the response (2–14 days of treatment) were significantly higher for combination therapy with IFN-α and ribavirin than for IFN-α monotherapy [20]. Therefore, the efficacy of combination therapy for patients with hepatitis C could be determined by serum HCV dynamics during the early stage of treatment, especially when HCV-RNA was undetectable in the early phase.

The mechanism of action of ribavirin in combined treatment for chronic HCV infection has been vigorously investigated [21]. At present, there are several proposed mechanisms of action of ribavirin [21–23]. Among them, we focused on the ability of the viral RdRp to utilize ribavirin triphosphate and to incorporate this nucleotide with reduced specificity, thereby mutagenizing the genome and decreasing the yield of infectious virus [6,21]. We then attempted to determine the relationship between viral RdRP sequence variations and responsiveness to IFN-α and ribavirin combination therapy by nucleic acid sequence analysis. The NS5B region coding RdRP consists of 591 amino acids. Direct sequencing of the NS5B region of HCV RNA from chronic hepatitis C patients with genotype 1b and high viremia clearly revealed that E124K and I85V were closely associated with early HCV clearance by combination therapy. The results of direct sequencing analysis showed that some nucleic acid residues were mixed in all patients, and that some quasispecies existed. However, the nucleic acid residues at the 85 and 124th positions of the RdRP were identical in each patient. Two patients previously treated with IFN-α monotherapy were included in this study: one patient (Pt3) has V85 and K124 in the HCV RdRP and the other (Pt7) had I85 and E124. The former was a good responder to IFN-α and ribavirin combination therapy, but the latter was not. This result indicates that I85V and E124K substitutions did not affect responsiveness of HCV to IFN-α monotherapy, and implies the direct or indirect participation of ribavirin in this responsiveness. Lohmann et al [24] identified four amino acid sequence motifs crucial for RdRP activity (residues 220–225, 282–291,317–319 and 342–346), and Qin et al [27] determined that motifs E18, Y191, C274, Y276 and H502 were critical for RdRP activity. As the 85 and 124th amino acid substitutions were not included in these motifs, and this did not affect the essential function of replication of HCV-RNA, HCV viral load was high in our patients before treatment. Neither the 85th nor the 124th position is related to either the β-loop (residues 445–454) or carboxyl- terminal tail (residues 545–569), interaction of which occludes the nucleic acid-binding site [25,27]. Like most nucleic acid polymerases, the RdRP of HCV has finger, palm, and thumb subdomains [25–27]. The 85 and 124th amino acids are located in helix D and helix F in the finger domain, respectively. Comparison of the tertiary structure model of HCV-BK (Protein Data Bank number 1QUV) [28] with that of HC-J4 (Protein Data Bank number 1NB6) [29] showed that the 85 and 124th amino acid substitutions do not cause significant conformational change (Fig. 3). For poliovirus RdRP, a single substitution at the 64th amino acid position in the finger domain confers resistance to ribavirin, as it increases fidelity of incorporation of substrates [30]. Pfeiffer et al [30] reported that a single mutation in poliovirus RdRP confers resistance to ribavirin. They proposed that a G64S substitution in the poliovirus RdRP affected the space for base mispair formation or reduced the flexibility of the finger domain. For HIV-1 reverse transcriptase, some studies have shown correlations between point mutations in nucleic acid-binding sites and fidelity [31–33]. In this study, the 85th amino acid of HCV RdRP was found to be distant from the active site, and substitution of isoleucine for valine yielded no change in polarity or charge. However, the 85th amino acid is located near the RNA primer binding site, and substitution of it may influence nucleotide misincorporation through slight rearrangement of the finger domain during polymerization. Since glutamic acid is an acidic amino acid and lysine a basic one, substitution at the 124th position is accompanied by a change in electrostatic potential on the surface of the protein, which may result in modulation of interaction of NS5B protein with other viral proteins (NS3, NS4A, NS4B and NS5A) [34–37] and/or host ones. Young KC et al has recently reported a ribavirin-resistant NS5B mutation of HCV during ribavirin monotherapy in five patients infected with HCV genotype 1a [38]. They reported that an NS5B amino acid 415 Phe-to-Tyr (F415Y) mutation emerged in all of the patients and presented this mutation as a ribavirin-resistant variant, using the HCV subgenomic replicon in Huh7 cells. This does not apply to our patients infected with genotype 1b, since their NS5B amino acid sequence had Y at position 415 before treatment. The effect of the amino acid substitution at NS5B85 and NS5B124 on HCV RNA replication is under investigation using the replicon system. In conclusion, our results suggest that the identified polymorphism in NS5B protein (E124K, I85V) is highly correlated with early viral clearance by combination therapy with IFN and ribavirin, and that its detection might be useful for prediction of clinical efficacy of IFN and ribavirin therapy for genotype 1b patients.

REFERENCES

1 Pol S, Nalpas B, Bourliere M *et al.* Combination of ribavirin and interferon-alpha surpasses high doses of interferon-alpha alone in patients with genotype-1b-related chronic – hepatitis C. *Hepatology* 2000; 31: 1338–1344.

2 Poynard T, McHutchison J, Goodman Z, Ling MH, Albrecht J. Is an 'a la carte' combination interferon alfa-2b plus ribavirin regimen possible for the first line treatment in patients with chronic hepatitis C? *Hepatology* 2000; 31: 211–218.

3 Saracco G, Ciancio A, Olivero A *et al.* randomized 4-arm multicenter study of interferon alfa-2b plus ribavirin in the treatment of patients with chronic hepatitis C not

responding to interferon alone. *Hepatology* 2001; 34: 133–138.
4 Fried MW, Shiffman ML, Reddy KR *et al.* Peginterferon alfa-2a plus ribavirin for chronic hepatitis C virus infection. *N. Engl. J. Med.* 2002; 347: 975–982.
5 Manns MP, McHuchinson JG, Gordon SC *et al.* Peginterferon alfa-2b plus ribavirin compared with interferon alfa-2b plus ribavirin for initial treatment of chronic hepatitis C: a randomized trial. *Lancet* 2001; 358: 958–965.
6 Crotty S, Maag D, Arnold J *et al.* The broad-spectrum antiviral ribonucleoside ribavirin is an RNA virus mutagen. *Nat Med* 2000; 6: 1375–1379.
7 Lanford RE, Guerra B, Lee H *et al.* Antiviral effect and virus-host interactions in response to alpha interferon, gamma interferon, poly(I)-poly(C), tumor necrosis factor alpha, and ribavirin in hepatitis C virus subgenomic replicons. *J Virol* 2003; 77: 1092–1104.
8 Bekkering FC, Brouwer JT, Leroux-Roels G, Vlierberghe HV, Elewant A, Schim W. Ultra rapid hepatitis C virus clearance by daily high-dose interferon in non-responders to standard therapy. *J Hepatol* 1998; 28: 960–964.
9 Zeuzem S, Lee JH, Franke A *et al.* Quantification of the initial decline of serum hepatitis C virus RNA and response to interferon alpha. *Hepatology* 1998; 27: 1149–1156.
10 Svensson JO, Bruchfeld A, Scvarcz R, Stahle L. Determination of ribavirin in serum using highly selective solid-phase extraction and high-performance liquid chromatography. *Ther Drug Monit* 2000; 22: 213–218.
11 Glue P. The clinical pharmacology of ribavirin. *Semin Liver Dis* 1999; 19 (Suppl. 1): 17–24.
12 Matteucci MD, Caruthers MH. Synthesis of deoxyoligonucleotides on a polymer support. *Biotechnology* 1981; 24: 92–98.
13 Kato N, Hijikata M, Ootsuyama Y *et al.* Molecular cloning of the human hepatitis C virus genome from Japanese patients with non-A, non-B hepatitis. *Proc Natl Acad Sci USA* 1990; 87: 9524–9528.
14 Sambrook J, Fitsch EF, Maniatis T. *Molecular Cloning: A Laboratory Manual.* NY: CSH Laboratory Press, 1990; 7–8.
15 Guex N, Peitsch MC. SWISS-MODEL and the Swiss-Pdb-Viewer: an environment for comparative protein modeling. *Electrophoresis* 1997; 18: 2714–2723.
16 Fried MW, Shiffman ML, Reddy KR *et al.* Peginterferon alfa-2a plus ribavirin for chronic hepatitis C virus infection. *N Eng J Med* 2002; 347: 975–982.
17 Buti M, Sanchez-Avila F, Lurie Y *et al.* Viral kinetics in genotype 1 chronic hepatitis C patients during therapy with 2 different doses of peginterferon alfa-2b plus ribavirin. *Hepatology* 2002; 35: 930–936.
18 McHutchison JG, Gordon SC, Schiff ER, Shiffman ML, Lee WM, Rustgi VK. Interferon alfa-2b alone or in combination with ribavirin as initial treatment for chronic hepatitis C. *N Eng J Med* 1998; 339: 1485–1492.
19 Ferenci, P, Brunner H, Nachbaur K *et al.* Combination of interferon induction therapy and ribavirin in chronic hepatitis C. *Hepatology* 2001; 34: 1006–1011.
20 Asahina Y, Izumi N, Uchihara M *et al.* A potent antiviral effect on hepatitis C viral dynamics in serum and peripheral blood mononuclear cells during combination therapy with high-dose daily interferon alfa plus ribavirin and intravenous twice-daily treatment with interferon beta. *Hepatology* 2001; 34: 377–384.
21 Lau JYN, Tam RC, Liang TJ, Hong Z. Mechanism of action of ribavirin in the combination treatment of chronic HCV infection. *Hepatology* 2002; 35: 1002–1009.
22 Tam RC, Pai B, Bard J *et al.* Ribavirin polarizes human T cell responses towards a type 1 cytokine profile. *J Hepatol* 1999; 30: 376–382.
23 Maag D, Castro C, Hong Z, Cameron CE. Hepatitis C virus RNA-dependent RNA polymerase (NS5B) as a mediator of the antiviral activity of ribavirin. *J Biol Chem* 2001; 276: 46094–46098.
24 Lohmann V, Korner F, Herian U, Bartenschlager R. Biochemical and structural analysis of the NS5B RNA-dependent RNA polymerase of the hepatitis C virus. *J Viral Hepat* 2000; 7: 167–174.
25 Bressanelli S, Tomei L, Roussel A *et al.* Crystal structure of the RNA-dependent RNA polymerase of hepatitis C virus. *Proc Natl Acad Sci USA* 1999; 96: 13032–13039.
26 Lesburg CA, Cable MB, Ferrari E, Hong Z, Mannarino AF, Weber PC. Crystal structure of the RNA-dependent RNA polymerase from hepatitis C virus reveals a fully encircled active site. *Nat Struct Biol* 1999; 6: 937–943.
27 Qin W, Yamashita T, Shirota Y, Lin Y, Wei W, Marakami S. Mutational analysis of the structure and functions of hepatitis C virus RNA-dependent RNA polymerase. *Hepatology* 2001; 33: 728–737.
28 Ago H, Adachi T, Yoshida A *et al.* Crystal Structure of the RNA-Directed RNA Polymerase of Hepatitis C Virus. *Structure (London)* 1999; 7: 1417–1426.
29 O'Farrell D, Trowbridge R, Rowlands D, Jager J. Substrate complexes of hepatitis C virus RNA polymerase (HC-J4): structural evidence for nucleotide import and de-novo initiation. *J Mol Biol* 2003; 326: 1025–1035.
30 Pfeiffer JK, Kirkegaard K. A single mutation in poliovirus RNA-dependent RNA polymerase confers resistance to mutagenic nucleotide analogs via increased fidelity. *Proc Natl Acad Sci USA* 2003; 100: 7289–7294.
31 Lewis DA, Bebenek K, Beard WA Wilson SH, Kunkel TA. Uniquely altered DNA replication fidelity conferred by an amino acid change in the nucleotide binding pocket of human immunodeficiency virus type 1 reverse transcriptase. *J Biol Chem* 1999; 274: 32924–32930.
32 Gutierrez-Rivas M, Menendez-Arias L. A mutation in the primer grip region of HIV-1 reverse transcriptase that confers reduced fidelity of DNA synthesis. *Nucleic Acids Res.* 2001; 29: 4963–4972.
33 Huang H, Chopra R, Verdine, Harrison SC. Structure of a covalently trapped catalytic complex of HIV-1 reverse transcriptase: implications for drug resistance. *Science* 1998; 282: 1669–1675.
34 Ishido S, Fujita T, Hotta H. Complex formation of NS5Bwith NS3 and NS4A proteins of hepatitis C virus. *Biochem Biophys Res Commun* 1998; 244: 35–40.
35 Piccininni S, Varaklioti A, Nardelli M, Dave B, Raney KD, McCarthy EG. Modulation of hepatitis C virus RNA-dependent RNA polymerase activity by the non-structural (NS) 3 helicase and the NS4B membrane protein. *J Biol Chem* 2002; 277: 45670–45679.

36 Shirota Y, Luo H, Qin W *et al.* Hepatitis C virus (HCV) NS5A binds RNA-dependent RNA polymerase (RdRp) NS5B and modulates RNA-dependent RNA polymerase activity. *J Biol Chem* 2002; 277: 11149–11155.

37 Dimitrova M, Imbert I, Kieny MP, Schuster C. Protein-protein interactions between hepatitis C virus nonstructural proteins. *J Virol* 2003; 77: 5401–5414.

38 Young KC, Lindsay KL, Lee KJ *et al.* Identification of a ribavirin-resistant NS5B mutation of hepatitis C virus during ribavirin monotherapy. *Hepatology* 2003; 38: 869–878.

Available online at www.sciencedirect.com
SCIENCE DIRECT
Hepatology Research 29 (2004) 97–103
Hepatology Research
www.elsevier.com/locate/ihepcom

Efficacy of non-invasive elastometry on staging of hepatic fibrosis

Hidetsugu Saito [a,*], Shinichiro Tada [a], Nobuhiro Nakamoto [a], Kumi Kitamura [a], Hitomi Horikawa [a], Satoshi Kurita [a], Yoshimasa Saito [a], Hirokata Iwai [b], Hiromasa Ishii [a]

[a] *Department of Internal Medicine, School of Medicine, Keio University, 35 Shinanomachi, Shinjuku-ku, Tokyo 160-8582, Japan*
[b] *Society of Highly Advanced Medical Technology, 4-1 Kioi-cho, Chiyoda-ku, Tokyo 102-0094, Japan*

Received 26 January 2004; received in revised form 2 March 2004; accepted 18 March 2004

Abstract

To assess the efficacy of elastmetry in the determination of fibrotic stage in the liver, we investigated correlation between liver histology and the elastometry using a device equipped with a vibrator and an ultrasound system (Echosens, Paris, France) in patients with chronic hepatitis C. Totally 75 patients, 24 in F1 stage, 17 in F2 stage, 18 in F3 stage, and 16 in F4 stage according to the new Inuyama classification without fatty change were investigated. Correlations between the staging of liver fibrosis and elastometry, serum fibrosis makers and platelet counts were investigated. The elastometry was absolutely non-invasive. Serum fibrosis markers did not well correlate with the stage of liver fibrosis. Platelet counts significantly ($P < 0.0001$) correlated with the fibrotic stage. Median platelet counts in each stage was; F1, 191.5; F2, 172.0; F3, 132.0; F4, 77.5 ($\times 10^3$ μl^{-1}). However, the deviation was comparatively broad. On the contrary, the elastometry correlated well to the stage of fibrosis and the deviation was small. Median elastometric levels in each stage were; F1, 6.25; F2, 7.80; F3, 13.85; F4, 34.00 (kPa). These results suggest that elastometry is significantly useful for evaluating fibrotic staging of the liver without any invasiveness.

Keywords: Fibrosis; Elasticity; Staging; Chronic hepatitis C; Non-invasive

1. Introduction

Fibrosis of the liver is a process of hepatic wound healing after continuous destruction of hepatocytes [1]. The major source of fibrogenesis is hepatic stellate cells (Ito cells), which transform from fat storing cells to fibroblasts and proliferate by some cytokines, such as transforming growth factor (TGF)-β [2], interleukin-13 [3], hepatocyte growth factor or angiotensin II [4,5]. Accumulation of collagen fibers and other extracellular matrix and regeneration of hepatocytes, that is, the scaring and regeneration, result in the formation of tissue change, liver cirrhosis, which progressively decreases hepatic function into chronic liver failure [6]. The progression of fibrotic change is always found in chronic viral infection and alcoholic liver diseases, but these produce different patterns of fibrosis as the disease progresses. These can be divided into those diseases that are portal-based and those that are acinar zone 3-based, and the portal-based diseases leading to cirrhosis include chronic viral hepatitis and zone 3-based diseases include alcoholic or non-alcoholic steatohepatitis.

Cirrhosis is not a static lesion and it may worsen, improve, or stay on, probably according to underlying disease activity. Recent studies revealed that the stage of fibrosis in chronic viral hepatitis C correlates to increased risk of hepatocarcinogenesis [7–11], and a success of anti-viral therapy results in decrease in both hepatic fibrotic stage and occurrence rate of hepatocellular carcinoma [11–13]. Thus, the regulation of hepatic fibrogenesis is important in the management of chronic liver diseases and evaluation of the stage of fibrosis in chronic hepatitis C is necessary for both diagnosis and treatment. Staging of the disease process in chronic hepatitis C indicates how far the disease has progressed in the course of its natural history, and at the same time how far the risk for developing liver cancer has impended. At the end stage, the disease has run its course and the patient dies

* Corresponding author. Tel.: +81-3-3353-1211; fax: +81-3-3351-8705.
E-mail address: hsaito@sc.itc.keio.ac.jp (H. Saito).

1386-6346/$ – see front matter © 2004 Elsevier B.V. All rights reserved.
doi:10.1016/j.hepres.2004.03.007

by liver failure or hepatocellular carcinoma. The establishment of the staging of liver diseases is always determined by liver biopsy.

Although the complete diagnosis of the stages of liver fibrosis can be determined in autopsy specimens, where entire liver can be carefully examined, needle biopsies are the main procedure for histologic evaluation in living patients. The needle biopsy is sometimes subject to sampling error, with small amount of samples [14,15]. Moreover, although needle biopsy is safe procedure, it sometimes makes complications such as pain, intra-abdominal bleeding, sampling from other organs, or penumothorax [16–18]. These conditions lead a new technology to make a non-invasive apparatus that can evaluate the soft tissue elasticity, which reflects fibrosis in the tissue, using a low-frequency shear wave and an echogram. The apparatus named Fibroscan® (Echosens Co., Paris, France) measures the elasticity of organs by measuring the velocity of a low-frequency shear wave going through the liver using transient elastography [19–21]. The speed of the wave was determined in any 2 cm in the liver from 2.5 to 6.5 cm depth from the surface. The elasticity of the liver is determined by the accumulation of fibrosis, so that the measurement of elasticity correlates to the degree of hepatic fibrosis. The aim of this study is to evaluate the usefulness of this apparatus, Fibroscan® (version 1), in the determination of hepatic fibrotic stage. To that effect, we examined the patients with chronic hepatitis C who had been biopsied within 3 month before and after the measurement with Fibroscan®, and we investigated the correlation between the elastometry and the staging of hepatic fibrosis according to the new Inuyama classification [22] that is the standard evaluating system in Japan.

2. Patients and methods

Patients with chronic hepatitis C and liver cirrhosis type C, who visited and received liver needle biopsy in our department in 2003 were included in this study after giving a well documentation of the purpose and methods of this study and having their acceptance for enrolling in this study. The patient received elastometry with Fibroscan® version 1 within 3 months before or after liver biopsy. The case in which fatty deposit of hepatocytes was found in more than 10% of whole hepatocytes in the sample was eliminated in this study because it has not been determined that fatty change might affect the result of elastometry.

The patient was laid on a bed on their backs and the location of measurement was determined with B-mode ultrasound. Elastometry was performed by contacting the probe of apparatus with a range of pressure at an intercostal area on the liver, and the measurement was done within a second after pushing the switch. The elasticity was automatically calculated in the apparatus and the data were shown as kilo Pascal (kPa). The elasticity of a patient was measured 10 times and the median measured level was automatically shown at the window and the result was printed after the measurement. On the same date, we measured serum fibrosis makers, the levels of type IV collagen 7S, type III procollagen-*N*-peptide (P-III-P) and hyarulonic acid, and also platelet counts. We investigated the correlation between the levels of elastometry, the stage of liver fibrosis, platelet counts, and serum fibrosis markers. The stage of hepatic fibrosis was determined by two experts of liver pathology without information of any clinical data according to the new Inuyama clacification [21]. Liver biopsy was performed with 16-gauge needle biopsy apparatus (TopNotch, Boston Scientific Japan Co., Tokyo, Japan).

3. Statistic analysis

The data of elastometry was automatically shown in the central value. The data of each fibrosis stage were calculated and indicated by mean ± standard deviation. The correlation between the data and the fibrosis stage was determined by Kruskal–Wallis analysis. The correlation between the data was determined by Mann–Whitney test.

4. Results

Totally 75 cases of chronic hepatitis C and liver cirrhosis type C were enrolled in this study. The age distributed from 18 to 74 and the central level was 50 year-old. The number of patients in each fibrotic stage was 24 in F1 stage, 17 in F2 stage, 18 in F3 stage, and 16 in F4 stage (liver cirrhosis).

The elastometry was entirely non-invasive and no one complained anything during and after the examination. The measurement was successful in almost all patients, but it did not work in patients with ascites, with narrow intercostal spaces, and with excess obesity. We tried to measure the elasticity of ex vivo liver from pig, but we could never measure it, suggesting that the chest wall is necessary for the measurement of hepatic elasticity with this apparatus.

The correlation between the elastometry and serum fibrosis makers was not found in this study. The median level (and 50% levels) of type IV collagen 7S in each fibrotic stage was F1, 4.1 ng/ml (3.5–4.1); F2, 4.4 ng/ml (4.2–4.5); F3, 4.9 ng/ml (4.0–5.4); F4, 9.4 ng/ml (7.3–22.5) (Fig. 1). Those of P-III-P were; F1, 0.60 U/ml (0.54–0.73); F2, 0.87 U/ml (0.74–0.91); F3, 0.75 U/ml (0.59–0.91); F4, 1.30 U/ml (0.98–1.60) (Fig. 2). Those of hyaluronic acid were F1, 37.2 ng/ml (20.9–51.5); F2, 48.3 ng/ml (38.1–59.0); F3, 62.3 ng/ml (55.9–83.5); F4, 412.0 ng/ml (317.3–1110.0) (Fig. 3). The statistical differences of type IV collagen 7S between F1 and F2, F2 and F3, F3 and F4, were $P = 0.135$, 0.972, and <0.0001, respectively. Those of P-III-P were $P = 0.068$, 0.401 and 0.0215, respectively. Those of hyaluronic acid were $P = 0.0545$, 0.051 and 0.0004, respectively. Thus, these serum fibrosis makers

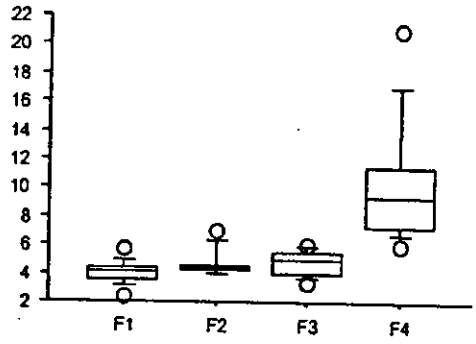

	Median level	P value
F1	4.10	P=0.135 (F1 vs. F2)
F2	4.40	P=0.972 (F2 vs. F3)
F3	4.90	P<0.0001 (F3 vs. F4)
F4	9.40	

Fig. 1. The median and 50% of the levels of serum type IV collagen 7S in each fibrotic stage of the New Inuyama Classification of chronic hepatitis C. The *P*-value in the table means the difference of levels between F1 vs. F2, F2 vs. F3, and F3 vs. F4, respectively, from the top. The significant difference was found in only between the levels of F3 and that of F4 ($P < 0.0001$).

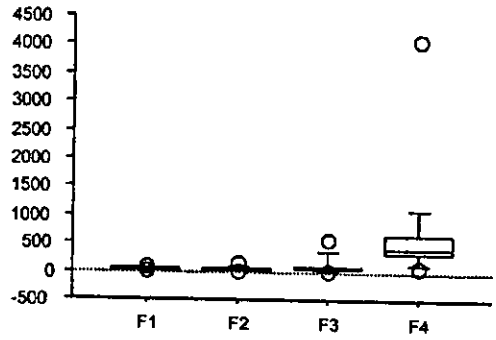

	Median level	P value
F1	37.2	P=0.055 (F1 vs. F2)
F2	48.3	P=0.051 (F2 vs. F3)
F3	62.3	P=0.0004 (F3 vs. F4)
F4	412.0	

Fig. 3. The median and fifty percent of the levels of serum hyaluronic acid in each fibrotic stage of the New Inuyama Classification of chronic hepatitis C. The *P*-value in the table means the difference of levels between F1 vs. F2, F2 vs. F3, and F3 vs. F4, respectively, from the top. The significant difference was found in only between the levels of F3 and that of F4 ($P = 0.0004$).

significantly increased in the fibrotic stage between F3 and F4, but they could not distinguish between F1 to F3.

On the other hand, platelet counts significantly ($P < 0.0001$) correlated with the fibrotic stage (Fig. 4). The median level of platelet counts (and 50% levels) in each stage was; F1, 191.5 × 10^3 μl^{-1} (173.0–235.5); F2, 172.0 × 10^3 μl^{-1} (145.0–203.0); F3, 132.0 × 10^3 μl^{-1} (104.5–163.0); F4, 77.5 × 10^3 μl^{-1} (67.0–107.0). However, the deviation was comparatively broad even the patients

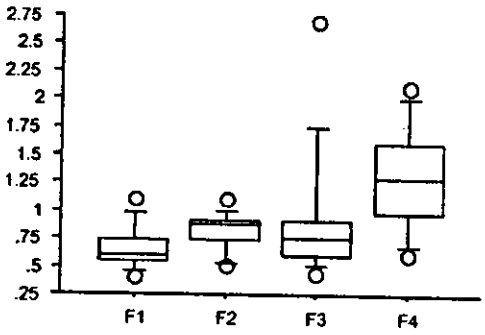

	Median level	P value
F1	0.60	P=0.068 (F1 vs. F2)
F2	0.87	P=0.401 (F2 vs. F3)
F3	0.75	P=0.022 (F3 vs. F4)
F4	1.30	

Fig. 2. The median and 50% of the levels of serum type III procollagen-*N*-peptide (P-III-P) in each fibrotic stage of the New Inuyama Classification of chronic hepatitis C. The *P*-value in the table means the difference of levels between F1 vs. F2, F2 vs. F3, and F3 vs. F4, respectively, from the top. The significant difference was found in only between the levels of F3 and that of F4 ($P = 0.022$).

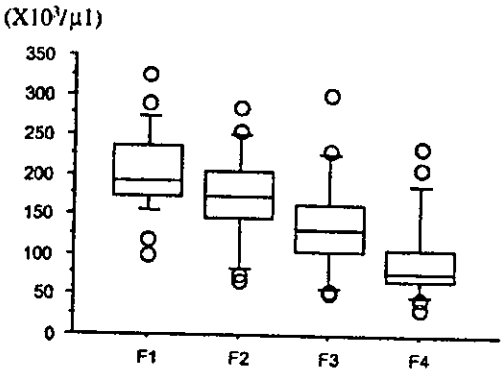

	Median level	P value
F1	191.5	P=0.068 (F1 vs. F2)
F2	172.0	P=0.048 (F2 vs. F3)
F3	132.0	P=0.020 (F3 vs. F4)
F4	77.5	

Fig. 4. The median and fifty percent of the levels of platelet counts in each fibrotic stage of the New Inuyama Classification of chronic hepatitis C. The *P*-value in the table means the difference of levels between F1 vs. F2, F2 vs. F3, and F3 vs. F4, respectively, from the top. The significant difference was found in between the levels of F2 and that of F3 ($P = 0.048$), and between F3 and F4 ($P = 0.020$).